# The effect of impact conditions on the wear and deformation behavior of wear resistant steels

Matti Lindroos[1)*], Vilma Ratia[1)], Marian Apostol[1)], Kati Valtonen[1)], Anssi Laukkanen[2)], Wolfgang Molnar[3)], Kenneth Holmberg[2)], and Veli-Tapani Kuokkala[1)]

[1)] Tampere Wear Center, Department of Materials Science, Tampere University of Technology, P.O. Box 589, FI-33101 Tampere, Finland
[2)] VTT Technical Research Centre of Finland, P.O. Box 1000, FI-02044 VTT Espoo, Finland
[3)] AC$^2$T research GmbH, Viktor-Kaplan-Straβe 2, AT-2700 Wiener Neustadt, Austria
[*]Corresponding author: matti.v.lindroos@tut.fi

## Abstract

The deformation and wear behavior of four high strength wear resistant steels were studied in various impact conditions to evaluate their performance in applications involving heavy impacts and impact-abrasion. In the normal direction impacts, the studies were conducted with single and repeated (multiple) drop tests. To better simulate the actual application conditions, the samples were positioned at an angle relative to the impact direction in the tests with the high velocity particle impactor (HVPI) device. The effect of strain rate was investigated using constant size projectiles made from materials with different density but keeping the impact energy constant by varying the incident projectile velocity. The effect of surface hardening on the wear resistance of the high strength steels was determined by impacting the same surface area multiple times at a constant velocity using spherical high velocity projectiles. Regardless of the rather similar hardness of the studied three martensitic steel grades, the impact behavior showed differences in wear rate and damage mechanisms in each case due to the microstructural characteristics of the materials. The adiabatic shear bands forming in the martensitic steels at higher loading rates were found to increase the wear rate. Moreover, the carbide reinforced steel performed in general better than the martensitic grades but showed more brittle behavior and generation of crack networks that can affect the wear performance of the material.

Keywords: High velocity impact; high strength steel; adiabatic shear bands (ASB); wear testing

Highlights:

- Deformation and wear behavior of high strength steels depends on the impact conditions
- Microstructural features affect the impact behavior more than the initial hardness
- Adiabatic shear bands increase the impact wear of auto-tempered martensitic steels

# 1 Introduction

The wear plates used in many demanding applications, such as mining, crushing and earth construction, have to withstand both abrasion and high energy impacts. Many commercially available quenched steels can provide the required resistance against abrasion due to their high surface hardness and also decent impact resistance enabled by the capability of the microstructure to absorb impact energy. For durable and lasting solutions in harsh wear conditions, more precise understanding of the effects of microstructure on the wear behavior is, however, still needed.

Despite numerous comprehensive studies on the behavior of wear resistant steels in abrasive conditions [1-4], the performance of these steels in the varying impact conditions has not been widely studied. Some studies consider also impact-abrasion or pure impact conditions, but are often restricted to relatively low energy impacts in laboratory scale experiments [6-13]. Higher energies have been used to investigate ballistic impacts, foreign object damage, and very high velocity impacts in a local scale, which can lead to drastic failures as compared to the common impact/erosive wear conditions [14-18]. This challenge is even more pronounced since high impact velocities are often used in laboratory experiments to reach the required impact energy with small impacting particle size. It would, however, be advisable to stay in the range of realistic conditions to avoid changes in the deformation mechanisms as compared with the in-service conditions. In addition, the small projectile size makes in-situ observations, such as tracking of the particles, more difficult as well as complicates the subsequent microstructural examinations due to the small wear crater sizes. The effects of material parameters, such as the work hardening capability, ductility and strength, on the wear behavior can be rather precisely determined in more controlled environments, which is not as straightforward in many laboratory wear experiments involving large amounts of particles and less control over the individual contacts [6-9]. Moreover, the controlled impact tests are excellent tools for producing the material data needed in the material models and numerical simulations, and well as in the validations of the results of the simulations.

The martensitic microstructure is often selected for its excellent abrasive wear endurance and reasonable impact resistance. Nevertheless, the wear rate can vary markedly depending on the wear conditions, such as the direction and velocity of the impact. The formation of wear particles also depends on the active deformation and failure mechanisms. Furthermore, the use of different strengthening or manufacturing methods to enhance the properties of the wear resistant steels can

affect also their wear behavior, when certain mechanical and microstructural limits are reached leading to the formation of wear particles [19].

Wear resistant steels are non-standardized steels with various quenched grades available. It has been found that the wear behavior of these steels can vary significantly even if they have similar hardness but different composition and manufacturing methods [20].

In this study, the wear and deformation behavior of four high strength wear resistant steels are investigated in three impact conditions, which cover the normal direction and two different oblique angle impact cases. Moreover, the relevance of impact energy, impact velocity, and number of impacts on the material behavior are discussed.

## 2. Materials and methods

### 2.1. Materials

Four high strength experimental wear resistant steels were investigated in varying impact conditions. Three of the steels were manufactured by thermomechanical rolling and direct quenching (DQ). They were alloyed slightly differently to enhance the properties such as strength, ductility and hardness needed for abrasive and impact resistance. These steels are generally used as wear resistant plates in highly abrasive and erosive applications, such as mining and earth construction. In the DQ process [37], the steels undergo auto-tempering leading to a microstructure containing a combination of tempered martensite and hard untempered martensite. Similar types of DQ steels manufactured in a laboratory scale rolling DQ process have shown quite good abrasive resistance [19]. The nominal compositions, hardness, and quasi-static and dynamic yield strengths of the steels are presented in Table 1. The volume contents of untempered martensite were approximated manually using image analysis on etched optical micrographs, where the untempered regions can be easily distinguished by their white color [20].

The martensitic microstructures of the studied steels differ in their prior austenite sizes, packet sizes, and block/lath sizes (Figure 1). The HV500A grade contained the least amount of finely dispersed untempered martensite. The slightly larger prior austenite size of the HV500B grade affected also the size of the untempered martensite packets, which appeared as larger islands in the microstructure. The fine microstructure of the HV550 grade consisted of plenty of fine and thin untempered regions. The hardest HV750 steel had a chromium carbide reinforced tempered

martensitic microstructure manufactured by casting. The hard and high strength HV750 is especially used in abrasive conditions that include occasional low and high energy impacts.

Table 1. Material properties and maximum nominal compositions of the studied materials.

| **Material** | **HV500A** | **HV500B** | **HV550** | **HV750** |
|---|---|---|---|---|
| **Microstructure** | Martensitic | Martensitic | Martensitic | Martensitic with $Cr_7C_3$ |
| **Untempered martensite [vol.%]** | 4.1 ± 0.3 | 9.0 ± 0.1 | 18.5 ± 1.4 | n/a |
| **Surface hardness [HV10]** | 500-510 | 490-515 | 540-565 | 740-760 |
| **Compressive yield strength**<br>**0.1 [1/s] [MPa]**<br>**3600 [1/s] [MPa]** | <br>1800<br>2000 | <br>1950<br>2160 | <br>2070<br>2270 | <br>2540<br>2740 |
| **C [%]** | 0.30 | 0.32 | 0.36 | 2.00 |
| **Si [%]** | 0.80 | 0.70 | 0.60 | n/a |
| **Mn [%]** | 1.70 | 1.50 | 1.00 | n/a |
| **Cr [%]** | 1.50 | 1.00 | 1.50 | 20.0 |
| **Ni [%]** | 1.00 | 2.00 | 2.50 | n/a |
| **Mo [%]** | 0.50 | 0.70 | 0.80 | n/a |
| **B [%]** | 0.005 | 0.005 | 0.005 | n/a |

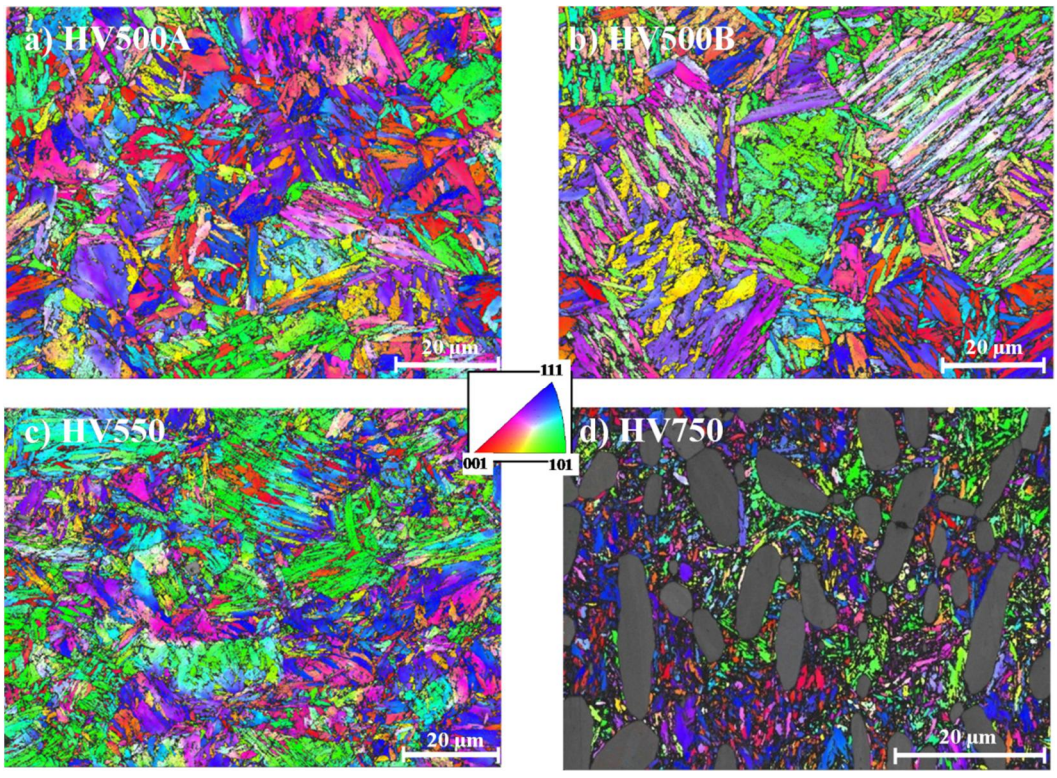


Figure 1. EBSD band contrast images overlaid with IPF-maps of the three different martensitic microstructures on the rolling plane a) HV500A, b) HV500B, and c) HV550, and d) the chromium carbide reinforced HV750 steel.

## 2.2. Experimental procedure

Various impact conditions were studied using oblique and normal direction impacts in three different kinds of experiments: normal direction impact tests, high velocity high strain rate (impulse) tests, and multiple impact tests. Table 2 summarizes the test procedures and the test variables used. The impact energies were chosen to range from 1 J to 17 J. In all experiments, the projectiles were ball bearing balls with a 9 mm diameter finished to grade 10, ISO 3290 [21]. Unlike in many previous studies, the size of the impacting particles was relatively large for laboratory scale tests. This allowed the use of more realistic impact velocities for higher energies and more distinctive deformation and wear analysis of the impact craters.

Table 2. Summary of the impact test methods and varied parameters.

| Method | Variable | Constants | Impact energy [J] | Impacts | Angle [°] | Strain rate |
|---|---|---|---|---|---|---|
| **Drop test** | Energy and impacts | Angle and impacts or energy | 1, 2, 5, 6 | Single/Multiple | 90 | Low |
| **Impulse test** | Rate of deformation | Energy and angle | 6, 17 | Single | 30 | High |
| **Multiple impacts test** | Impacts | Energy and angle | 17 | Multiple | 30 | Moderate |

### 2.2.1. Normal direction impact tests

The normal direction drop experiments were conducted with a single impact test (SIT) device at the $AC^2T$ Research GmbH. The SIT device consists of a sledge, a guiding slide, and a sample holder platform. The impact energy and momentum can be changed by altering the weight added to the sledge and its dropping height. A tungsten carbide cobalt (WC-Co) ball impactor was used so that the impact was delivered to the material through the ball. Before the drop, the sledge was secured with a trigger to a predetermined height, from which it was then released. This enabled an accurate adjustment of the dropping height. The angle of the impact was perpendicular to the sample surface.

In the test series, the impact energies were 1, 2, 5, and 6 J in the single impacts. In addition, multiple impacts were investigated with a constant 6 J energy up to 10 impacts. The impacting mass was 2.0 kg, and the impact energy was varied with the dropping height. Every drop test was conducted with three repetitions to provide basic statistics for the data. The typical impulse values during the drop tests varied between 2 and 5 Ns.

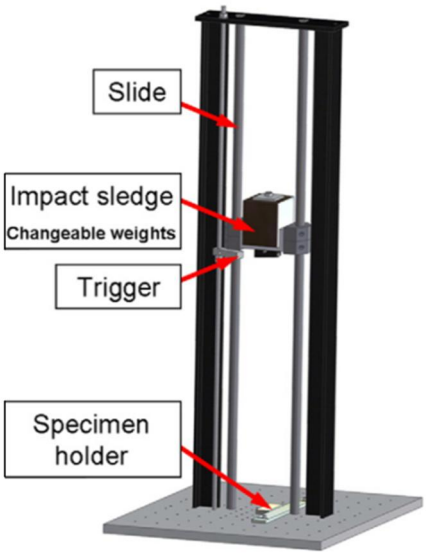


Figure 2. Schematic of the single impact tester at AC$^2$T Research GmbH [13].

### 2.2.2. High velocity impact tests

The single and multiple angular impact tests were carried out using the high velocity particle impactor (HVPI) at the Tampere Wear Center [22-24,35,36]. The device, which is schematically presented in Figure 3, fires a single particle with a smooth bore compressed air gun towards the sample, which in the present tests was placed at a 30 degree angle with respect to the projectile. To determine the projectile's initial kinetic energy prior to the impact, the incident velocity was measured by a commercial chronometer placed in front of the target assembly. The impact event was recorded with a high speed camera system, which allows calculation of the residual kinetic energy with an image analysis. Two high speed images were superimposed and the distance traveled was determined with respect to the time consumed to derive the exit velocity. The energy dissipation in the oblique impacts was calculated from the loss of the kinetic energy during the impact using Equation 1, where $m_p$, $v_i$, $v_e$ are the mass and incident and exit velocities of the projectile, respectively.

$$E_d = 0.5\, m_p(v_i - v_e)^2 \quad (1)$$

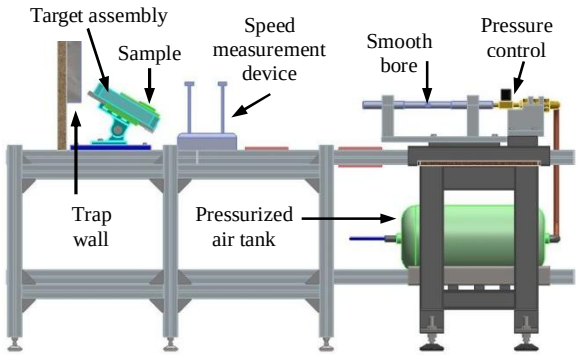


Figure 3. Schematic of the high velocity particle impactor at Tampere Wear Center.

In the single impact tests, the effect of the deformation rate on impact wear was studied by launching the impact projectiles at varying velocities. The use of different projectile materials allowed a change in the impact velocity while keeping the impact energy and projectile volume and shape constant. The heaviest projectile was a similar WC-Co cemented carbide ball as in the SIT tests. Higher impact velocities were needed to gain the same impact energy with the lighter ceramic projectiles, zirconia ($ZrO_2$) and silicon nitride ($Si_3N_4$). Table 3 lists the material parameters and the target impact velocities for the two impact energies used in the experiments.

Table 3. Material parameters and target impact velocities used in the experiments.

| **Ball material** | **Density [g/cm$^3$]** | **Projectile mass [g]** | **Hardness HV10** | **Impact velocity [m/s]** | |
|---|---|---|---|---|---|
| | | | | **6 J** | **17 J** |
| **WC-Co cemented carbide** | 14.95 | 5.69 | 1800 | 46 | 77 |
| **Zirconia $ZrO_2$** | 5.70 | 2.22 | 1240 | 72 | 122 |
| **Silicon nitride $Si_3N_4$** | 3.21 | 1.24 | <1600 | 98 | 165 |

In multiple impact tests, the constant incident energy was 17 J, of which roughly 34-40% was consumed during the impact depending on the test material. The impulse (Ns) values were roughly 100-200 times smaller than the ones in the drop tests. The test materials were impacted at a constant velocity for 1, 2, 5, 10 and 20 times. All samples were polished prior to the experiments.

## 2.3. Profiling and characterization

The surface topologies of the impact craters were analyzed using a Plμ confocal imaging profilometer and a Wyko NT-1100 optical profilometer. The profilometer data was used to calculate

the volume losses inflicted by the impacts and to determine the cutting-to-plasticity ratios. The cutting-to-plasticity ratio was defined as

$$\varphi = \frac{|V_{neg}| - |V_{pos}|}{|V_{neg}|} \tag{2}$$

where $V_{neg}$ is the negative volume below the original sample surface and $V_{pos}$ is the positive volume above the zero level. The values of φ range from 0 to 1, so that 1 means that all material has been cut off, while 0 denotes only ideal plastic flow of the material without any actual material removed or lost. Figure 4 shows a quarter of a typical 3D profile after a normal direction impact.

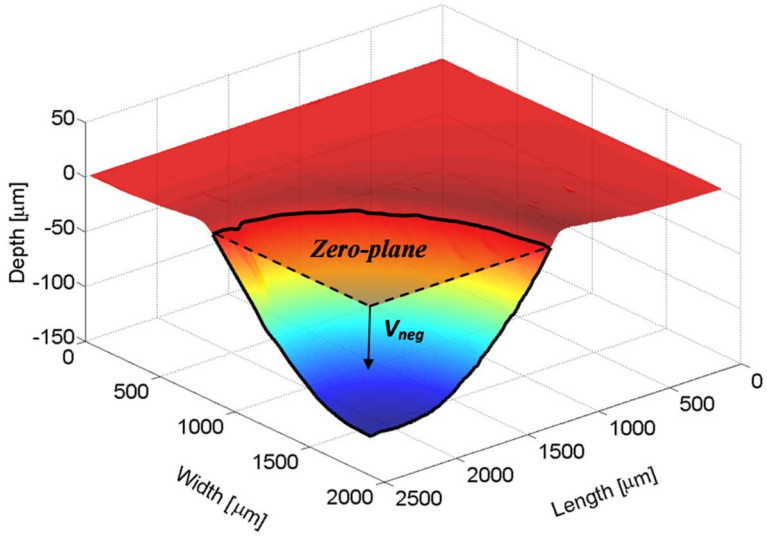


Figure 4. 3D profile of the crater after a normal direction impact. Above the zero-plane, the volume is considered to be positive $V_{pos}$.

As shown in Equation 3, the amount of wear per dissipated energy during the contact was calculated making use of the volume loss obtained from the 3D profilometer data and the measured incident and reflected velocities of the projectile.

$$\frac{W}{E_d} = \frac{|V_{neg}| - |V_{pos}|}{0.5\, m_p (v_i - v_e)^2} \tag{3}$$

# 3. Results

## 3.1 Normal direction impact tests

The effect of impact energy on the wear and deformation in a single impact was studied with four different energies. The wear results of single impact experiments in Figure 5 show quite linear behavior as a function of the impact energy. For all materials, the volume loss doubled when the impact energy increased from 3 J to 6 J. On the other hand, the cutting-to-plasticity ratio varied from 0.6 to 0.8 depending on the impact energy and the tested steel. For the HV500 grades, the value increased with increasing impact energy, while for the HV550 and HV750 steel grades the ratio remained essentially at 0.7. The wear results showed that initially higher quasi-static and dynamic strengths do not directly imply less wear, as seen for example in the comparison between the HV500A and HV500B data. However, the volume loss of the high strength HV750 carbide reinforced steel was approximately 40-50% less than that of the martensitic grades.

Figure 6 presents the bottom of a typical impact crater seen in the martensitic grades. The material is both plastically displaced as well as removed by several mechanisms. In this case, the edges of the crater do not show significant amounts of piled-up material, which indicates there to be more removal (cutting) than pure displacement. Circumferential cracks appear around the crater alongside with visible adhesive damage. The small loose particles in the bottom and the light scratches also suggest slight scuffing type wear. Some but not significant amounts of material had also adhered to the ball surface.

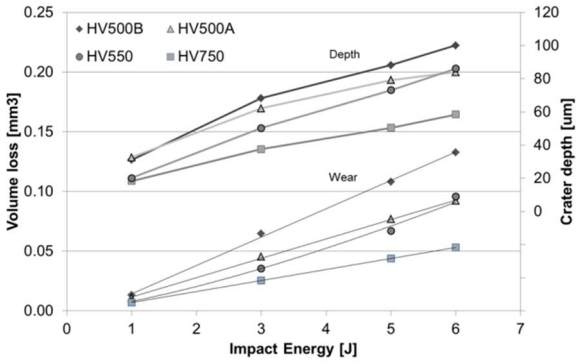


Figure 5. Effect of impact energy on the deformation and wear in the normal direction impacts.

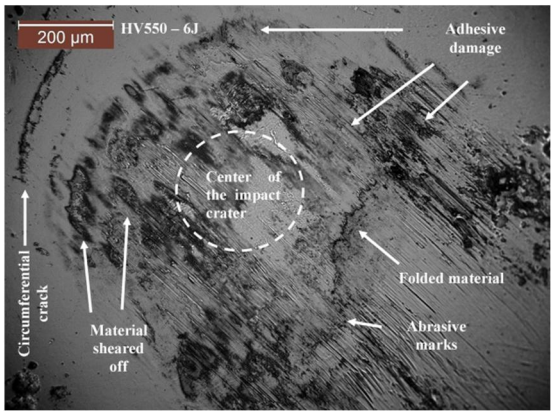


Figure 6. Typical damage and material removal mechanisms observed in the impact crater in an HV550 specimen after a single 6 J impact.

The effect of multiple impacts was also investigated using a constant impact energy of 6 J up to ten impacts. Figure 7 presents the effect of multiple impacts conducted in the same area on the volume loss of the steels. The accuracy and repeatability of the test device is very good and the impacts hit the same location with good precision. Thus, the experiments simulate well surface hardening and possible initiation of failure in cyclic impact loading. Figure 8 presents typical 2D profiles of the impact craters after ten impacts. As the height and shape of the pile-ups on the edges of the crater did not show constant geometry, the volume loss was approximated from the 3D profiles, which takes better into account the actual volumetric changes caused by the impacts.

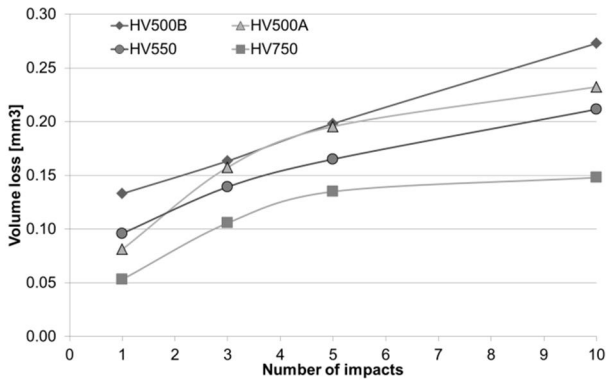


Figure 7. Volume loss of the tested steels after several impacts in the normal direction.

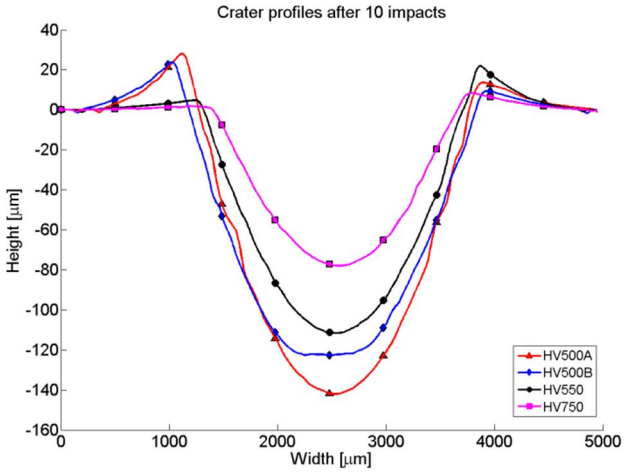


Figure 8. Crater profiles after ten impacts showing slightly uneven deformation.

All studied steels showed quite high cutting-to-plasticity ratios, between 0.7 and 0.8, after ten impacts. However, wear did not occur by the typical cutting mechanism, i.e., material shearing off by abrasives or by oblique impacts, but it was rather removed by adhesion and fracture of the deformed surface due to the impacts performed in the normal direction.

## 3.2 The effect of impact velocity in angular impacts

High velocity impact tests were conducted with the HVPI device to study the effect of strain rate (impulse) at constant energies on the investigated steels. Figure 9 presents the amount of volume loss exhibited by the test materials under high impact velocities at two different impact energies. The figure shows that when the impact energy is kept constant, the increase in the impact velocity increases wear in all studied steel grades used in the tests. With the higher impact energy of 17 J, it also appears that the wear rate of the martensitic steels saturates at a more or less constant level when the impact velocity approaches 150 m/s. In the 6 J tests, wear increases quite consistently with the impact velocity which, however, does not exceed 100 m/s in any of the tests. With the martensitic steels, the material removal rates with zirconia and silicon nitride projectiles requiring higher velocities to produce the pre-determined kinetic energies are increased by 50-100% when compared to the heavier and lower velocity WC-Co projectile. In turn, with the carbide reinforced HV750 steel the effect of impact velocity on wear is not so drastic.

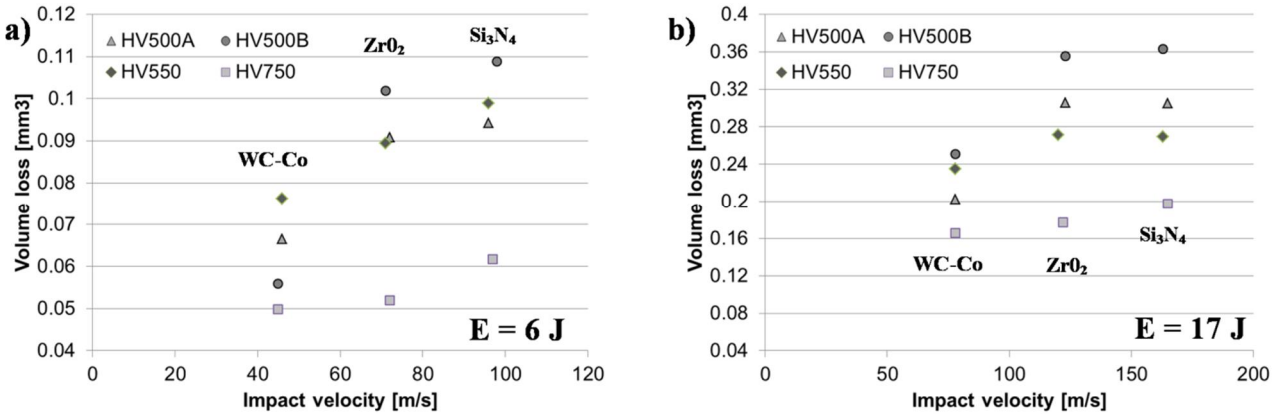


Figure 9. Effect of impact velocity at the constant energies of a) 6 J or b) 17 J on the volume loss of the studied steels.

The relative amounts of the energy dissipated during the impacts depended both on the sample and projectile materials. In the experiments with the WC-projectiles, 34-40% of the initial energy was dissipated in the impact, while the zirconia projectiles lost 24-32% and the silicon nitride projectiles 28-34% of their initial energy in the impact. These results could be linked to the slightly different frictional conditions between the balls and the sample surfaces or to the different mechanical properties of the projectiles.

The change in the deformation mechanism can be seen as an increase in the cutting-to-plasticity ratios. As shown in Table 4, when the impact velocity is increased, cutting in HV500 and HV550 steels increases, while HV750 with a different microstructure seems to be in this sense quite insensitive to the impact velocity. However, some subsurface crack networks were observed. Also, overall HV750 exhibits more cutting than plastic deformation compared with the other studied steels.

Table 4. Cutting-to-plasticity ratios of the studied materials with three different projectiles.

| **Impact energy** | **6 J** | | | **17 J** | | |
|---|---|---|---|---|---|---|
| **Material** | **WC** | **Zr0$_2$** | **Si$_3$N$_4$** | **WC** | **Zr0$_2$** | **Si$_3$N$_4$** |
| **HV500A** | 0.55 | 0.60 | 0.66 | 0.50 | 0.62 | 0.60 |
| **HV500B** | 0.46 | 0.73 | 0.73 | 0.52 | 0.74 | 0.74 |
| **HV550** | 0.58 | 0.70 | 0.72 | 0.72 | 0.67 | 0.6 |
| **HV750** | 0.75 | 0.75 | 0.77 | 0.69 | 0.75 | 0.74 |
| **Target velocities [m/s]** | 46 | 72 | 98 | 77 | 122 | 165 |

## 3.3 Wear and deformation in multiple angular impacts

The capability of the studied steels to resist wear and absorb impact energy in the surface hardened conditions was investigated with multiple oblique angle impact experiments using the HVPI device. Figure 10 shows that the volume losses increased rather steadily throughout the tested range of 20 impacts. However, the cutting-to-plasticity ratios seemed to saturate after the first impacts, remaining between 0.5…0.6 for the martensitic grades and between 0.6…0.7 for the carbide reinforced steel.

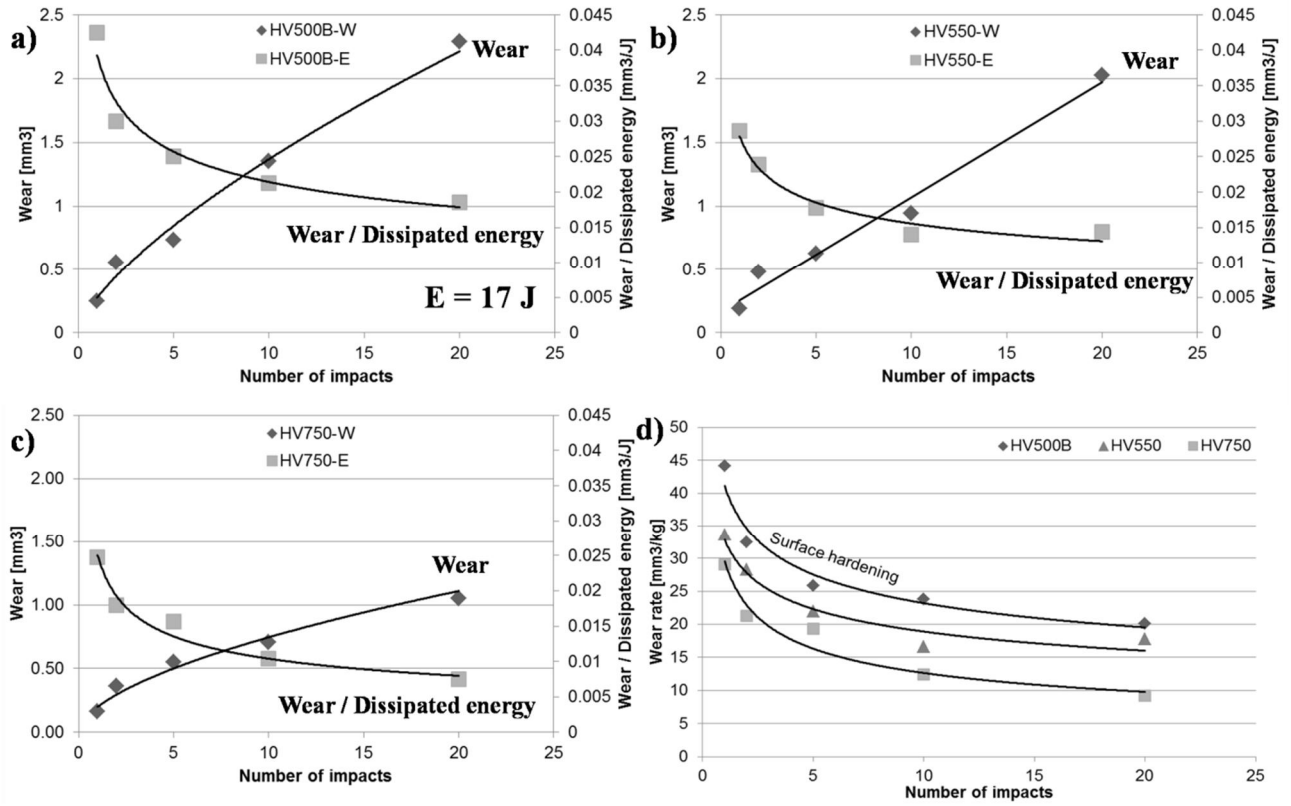


Figure 10. Effect of multiple impacts on the wear and wear/dissipated energy of the high strength steels during 30 degree impacts with a constant 17 J impact energy, a) HV500B, b) HV550, c) HV750, and d) the wear rates defined as volume loss/kilogram of impacting particles.

To compare the wear behavior of materials with different microstructures, including the some of the materials in different deformed states, the wear rate can be presented as wear per dissipated energy during impacts. It should be noted that energy will go also to other processes than wear during the impact event (e.g, friction). The energies dissipated during the impact were individually calculated from the high speed images of each test. Presentations of the wear rates based on the dissipated energy and the erosive particle mass produced quite similar results, which mean that the amount of

dissipated energy during consecutive impacts did not change markedly despite hardening of the target material. The consumed energy remained also essentially the same for all steels, between 34-40%. Consequently, even though the surfaces deformed plastically and hardened during the impacts, they did not show distinctive signs of a change in their ability to absorb energy. When comparing the volume loss results from ten-impact HVPI tests to the ones obtained from the drop tests, it can be noted that the wear is approximately 4-6 times more severe in the oblique angle HVPI tests. Interestingly, the cutting-to-plasticity ratios were approximately 0.2 higher (e.g., increased from 0.5 to 0.7) in the normal direction impacts but, on the other hand, the volumes displaced in the angular impacts were a magnitude larger.

Figure 11 shows the deformed craters after 20 constant energy impacts. The HVPI setup has quite good accuracy and it produces crater areas large enough to properly simulate impact wear. It is actually beneficial to aim impacts also partly to the ploughed regions of the crater to better understand the failure mechanisms and wear occuring also in the previously deformed regions. The martensitic grades had deformed plastically and generated shear lips at the exit side of the crater in the impact direction. Material had also folded in layers by deformation during repeated impacts, leading to subsurface shear localization that can be seen in the deformed craters. The layers were then prone to cutting off in the process, as shown by the small partly detached particles in the region (Figs. 11b and 12b). The shape of the crater in the HV750 steel (Fig. 11c) suggests that it has experienced more cutting than pure plastic deformation and that the material has been removed by shearing of wear particles from the surface. Moreover, the surface also contains small cracks in the matrix that may have propagated and released wear particles during the continued impacts.

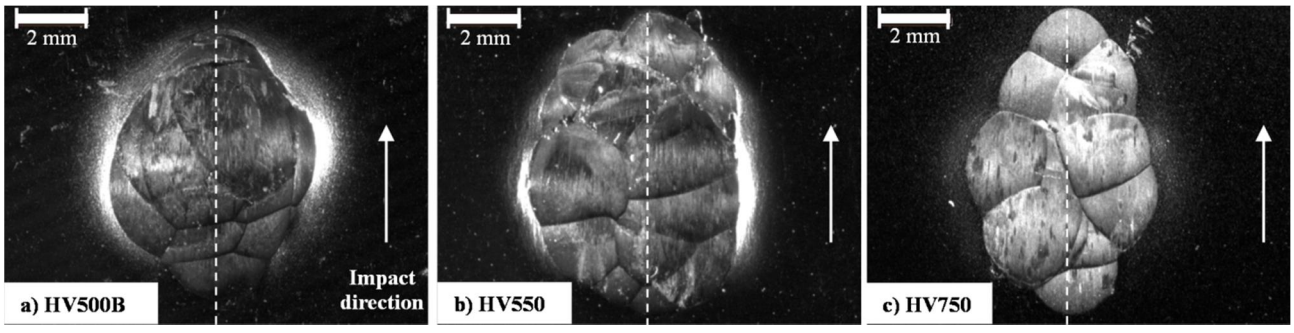


Figure 11. Surface of the wear craters after 20 impacts at 17 J impact energy with a WC-Co ball.

The cross-sectional study showed that the two martensitic grades exhibit also adiabatic shear banding (ASB) in the heavily deformed regions (Fig. 12). A concurrent failure mechanism, which is not directly related to the white shear bands, was seen either as a surface or subsurface shear crack

formation in the steels. A white layer, roughly 10 µm in thickness, was observed also on the surface of the martensitic grades. Similar adibatic shear bands and white surface layers were previously observed in both high strain rate mechanical tests and single impact experiments [27]. It is possible that it is a remnant of a previous shear band and/or partly formed by adhesive wear. Below the white surface layer some mechanical fibering of martensite was also observed in the shear directions.

In the HV750 steel, the fractures were mainly propagating between the carbides in the matrix, but also several fractured carbides were found. Moreover, extensive crack networks were developed in the deformed volume below the surface, making the steel susceptible also to fatigue wear.

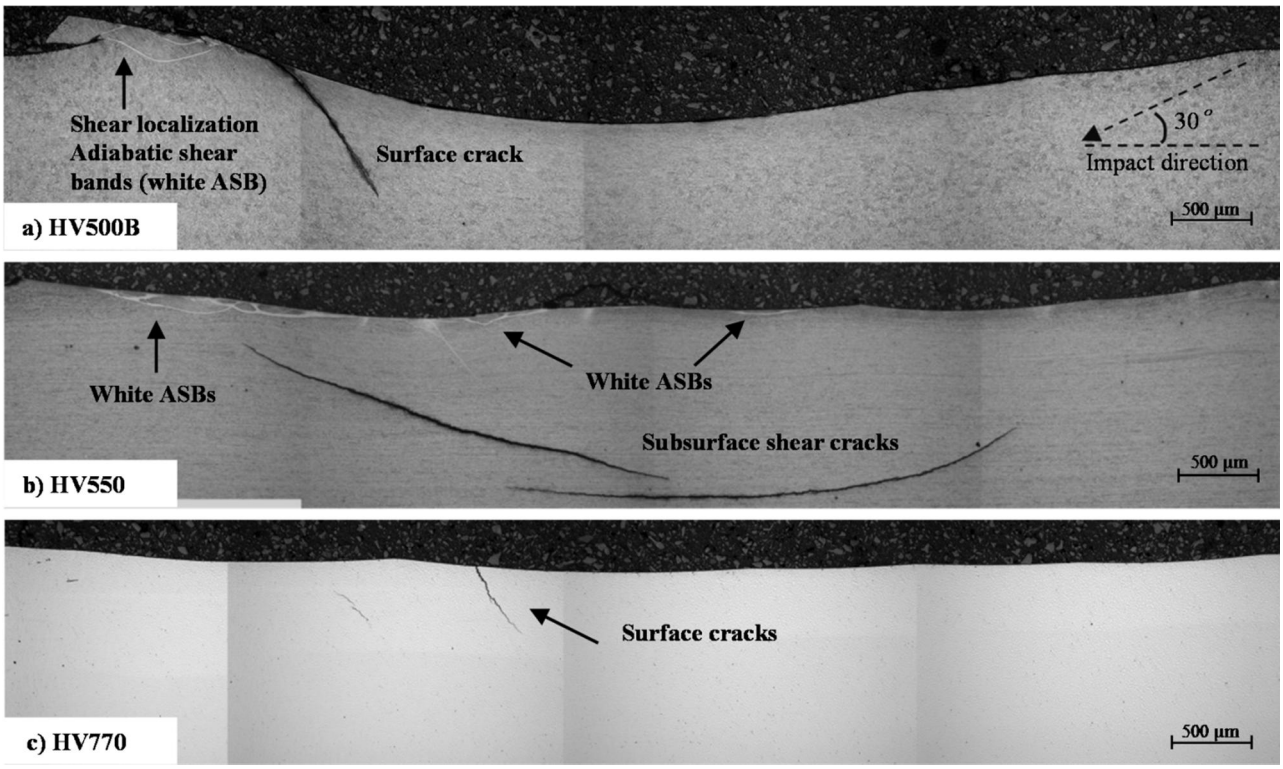


Figure 12. Cross-sectional views of the wear damage in the high strength steels after 20 impacts at 30 degrees with a constant impact energy of 17 J.

## 4. Discussion

The deformation and wear behavior of four high strength wear resistant steels were investigated in three impact conditions including the normal direction and two different oblique angle impact cases. Figure 13 schematically summarizes the main characteristics of the impact tests and the effects of the test conditions on the wear behavior of the studied steels.

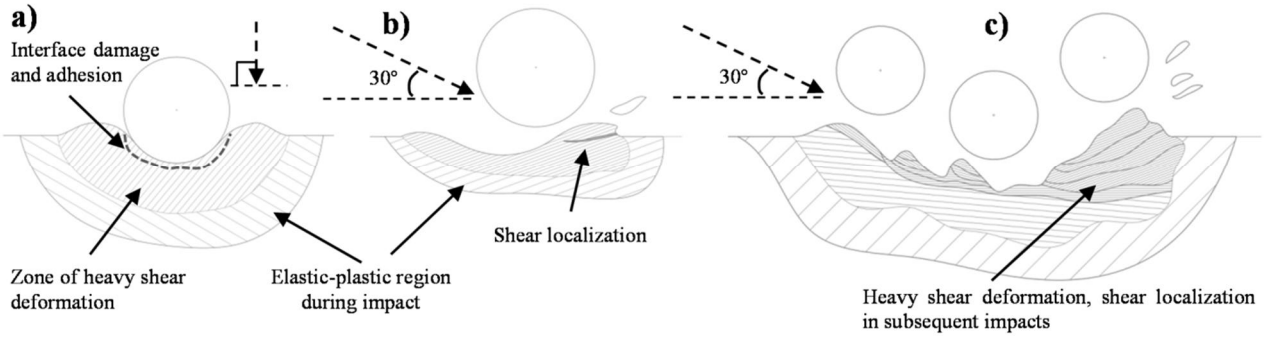


Figure 13. Impact deformation and wear characteristics of the high strength steels in the studied conditions, a) normal direction impact, b) oblique impact at different velocities, c) multiple oblique impacts.

If impact wear is formulated according to typical erosion models [25,26] and described as the unit energy required to remove material, it can be decomposed to a cutting part, which occurs usually in the lower angle impacts, and to a deformation part, which is more related to the high angle impacts. It is also generally acknowledged that the impact velocity affects the deformation mechanisms in the materials. The martensitic wear resistant steels have an additional tendency to adiabatic shear banding at high strain rates, which has been found to have some dependence also on the angle and energy of the impact [27,28]. In this study, clear evidence was found that the impact velocity and thus the strain rate have an increasing effect on the wear of the studied high strength steels.

Based on the observed wear behavior, two main failure mechanisms were found to be responsible for the material removal during the angular impacts. When the impact velocity was increased but the energy was kept constant, the martensitic steels showed increased cutting related to adiabatic shear banding. After multiple angular impacts, the steels also showed surface and subsurface shear fractures as a second mechanism. From the application point of view, it is worth to note that in some cases the formation of cracks may also be beneficial as they can absorb impact energy without critical failure, as seen in the current experiments.

The initial hardness and yield strength cannot solely explain the impact wear behavior of the martensitic steels. For example, the content of untempered martensite and the martensite morphology were found to affect the deformation and failure behavior of these steels. An increase in the untempered martensite content combined with small martensite block size resulted in high strength and good resistance against deformation, but at the same time the steels became more

susceptible to cutting fractures.

It has been shown [9,29] that in some cases the martensitic grades have lower wear resistance compared to the pearlitic and bainitic grades due to their limited strain hardening capability. In the current study, the effects of plastic deformation on the wear behavior became more clearly observable with increasing number of impacts, and it seems that in high angle impacts the surface of the steels work hardened in such a manner that the volume losses decreased considerably. Similar hardening behavior has been observed in martensitic steels in long-term impact-fatigue experiments [30]. Moreover, previous studies [27,31] have shown that the relatively good work hardening ability of martensitic wear resistant steels, exhibiting over 30-50% increase in hardness from the initial values, is likely due to their partially auto-tempered microstructure.

The characterization of the wear surfaces revealed that during oblique angle impacts material was removed especially from the piled-up regions formed in front of the impacting particles. Shear deformation had localized in these regions and produced both deformed and white adiabatic shear bands [27], which have also earlier been related to impact failures [32-34]. The results suggest that if the rate of deformation is increased, the investigated martensitic steels become more vulnerable to shear localization, which in turn increases the wear rates.

When comparing the studied martensitic steels with each other, the HV550 grade has the finest martensite lath size combined with the approximated highest content of untempered martensite, which produces the highest quasi-static and dynamic yield strength. However, the capability of the material to store energy during impacts is affected by many microstructural features, such as the martensite morphology, which as an example was seen in the current results when the cutting-to-plasticity ratios were evaluated.

## 5. Conclusions

The wear and deformation behavior of three auto-tempered martensitic steels with hardness in the range of 500-550HV, and a 750HV chromium carbide reinforced steel were studied in three different impact conditions including normal direction drop tests and high velocity angular impact tests with the HVPI device.

- Strain hardening of the steels enhances their wear resistance in repeated loading conditions in both normal and oblique impacts. At the same time, the steels do not show any notable signs of decreasing energy absorption capability based on the measured wear/dissipated energy values, even when some cracks or adiabatic shear bands appear in the oblique angle impact experiments.

- Adiabatic shear bands can increase the wear rate of the studied steels by as much as 50-100 % in single impacts, when the impact velocity is increased. Similar ASB development is observed also in the multiple oblique angle impact tests, which seems to promote the development of wear particles in long-term erosion by fracturing inside the ASB's.

- The HV750 carbide reinforced steel shows the best overall wear performance and oblique and normal angle impact resistance. It was, however, found to be prone to crack initiation and propagation in multiple high energy and single high velocity oblique impacts, which may restrict its use in high energy impact environments. Although the 500-550 HV martensitic grades were also found to develop adiabatic shear bands and suffer from surface initiated cracks in the above mentioned conditions, in impact-abrasion conditions they may endure longer than their harder carbide reinforced counterparts due to their higher ductility.

## Acknowledgements

The study was a part of the FIMECC DEMAPP programme funded by Tekes and the participating companies. Virpi Kupiainen is gratefully acknowledged for conducting profilometry at VTT Research Center of Finland. AC$^2$T research GmbH is thanked for collaboration and the possibility to use the SIT testing facilities.

## References

[1] J. Terva, T. Teeri, V-T. Kuokkala, P. Siitonen, J. Liimatainen, Abrasive wear of steel against gravel with different rock-steel combinations, Wear 267. (2009) 11, 1821-1831.

[2] J. Rendon, M. Olsson, Abrasive wear resistance of some commercial abrasion resistant steels evaluated by laboratory test methods, Wear. 267 (2009), 2055–2061.

[3] A.K. Jka, B.K. Prasad, O.P. Modi, S. Das, A.H. Yegneswaran, Correlating microstructural features and mechanical

properties with abrasion resistance of a high strength low alloy steel, Wear. 254 (2003), 120-128.

[4] S. Das Bakshi, P.H. Shipway, H.K.D.H. Bhadeshia, Three-body abrasive wear of fine pearlite, nanostructured bainite and martensite, Wear. 308 (2013), 46-53.

[5] R.D. Wilson, J.A. Hawk, Impeller wear impact-abrasive wear test, Wear. 225-229 (1999), 1248–1257

[6] V. Ratia, K. Valtonen, A. Kemppainen, V-T. Kuokkala, High-stress abrasion and impact-abrasion testing of wear resistant steels, Tribology Online. 8 (2013) 2, 152-161.

[7] V. Ratia, K. Valtonen, V-T. Kuokkala, Impact-abrasion wear of wear-resistant steels at perpendicular and tilted angles, Proceedings of the Institution of Mechanical Engineers, Part J: Journal of Engineering Tribology. 227 (2013) 8, 868-877.

[8] V. Ratia, I. Miettunen, V-T. Kuokkala, Surface deformation of steels in impact-abrasion: the effect of sample angle and duration, Wear. 301 (2013), 94-101.

[9] A. Sundström, J. Rendon, M. Olsson, Wear behavior of some low alloyed steels under combined impact/abrasion contact conditions, Wear. 250 (2001), 744-754.

[10] T. Slatter, R. Lewis, A.H. Jones, The influence of induction hardening on the impact wear resistance of compacted graphite iron (CGI), Wear. 270 (2011), 302-311.

[12] H. Rojacz, M. Hutterer, H. Winkelmann, High temperature single impact studies on material deformation and fracture behaviour of metal matrix composites and steels, Materials Science and Engineering A. 562 (2013), 39-45.

[13] H. Rojacz, G. Mozdzen, H. Winkelmann, Deformation and strain hardening of different steels in impact dominated systems, Materials Characterization. 90 (2014), 151-163.

[14] A. Rusinek, J.A. Rodríguez-Martinez, R. Zaera, J.R. Klepaczko, A. Arias, C. Sauvelet, Experimental and numerical study on the perforation process of mild steel sheets subjected to perpendicular impact by hemispherical projectiles, International Journal of Impact Engineering. 36 (2009), 565-587.

[15] X. Wang, J. Shi, Validation of Johnson-Cook plasticity and damage model using impact experiment, International Journal of Impact Engineering. 60 (2013), 67-75.

[16] G. Sundararajan, P. G. Shewmon, The oblique impact of a hard ball against ductile, semi-infinite target materials – Experiment and analysis, International Journal of Impact Engineering, 6 (1987) 1, 3-22.

[17] L.E. Murr, A.C. Ramirez, S.M. Gaytan, M.I. Lopez, E.Y. Martinez, D.H. Hernandez, E. Martinez, Microstructure

evolution associated with adiabatic shear bands and shear band failure in ballistic plug formation in Ti-6Al-4V targets. Materials Science and Engineering A. 516 (2009), 205-216.

[18] A.A. Cenna, K.C. Williams, M.G. Jones, Analysis of impact energy factors in ductile materials using a single particle impact test on gas gun, Tribology International 44 (2010), 1920-1925.

[19] E. Kinnunen, I. Miettunen, M. Somani, D. Porter, P. Karjalainen, I. Alamattila, A. Kemppainen, T. Liimatainen, V. Ratia, Development of A New Direct Quenched Abrasion Resistant Steel, International Journal of Metallurgical Engineering. 1 (2013), 27-34

[20] N. Ojala, K. Valtonen, V. Heino, M. Kallio, J. Aaltonen, P. Siitonen, V-T. Kuokkala, Effects of composition and microstructure on the abrasive wear performance of quenched wear resistant steels, Wear 317 (2014), 225-232.

[21] ISO standard 3290-1:2008, Rolling bearings — Balls — Part 1: Steel balls.

[22] M. Apostol, V-T. Kuokkala, A. Laukkanen, K. Holmberg, R. Waudby, M. Lindroos, High velocity particle impactor – Modeling and experimental verification of impact wear test. World Tribology Congress WTC 2013, Turin, Italy Sept 8-13. 2013.

[23] E. Sarlin, M. Apostol, M. Lindroos, V-T. Kuokkala, J. Vuorinen, T. Lepisto, M. Vippola. Impact properties of novel corrosion resistant hybrid structures, Composite structures. 108 (2014) 886-893.

[24] E. Sarlin, M. Lindroos, M. Apostol, V-T. Kuokkala, J. Vuorinen, T. Lepisto, M. Vippola, The effect of test parameters on the impact resistance of a stainless steel/rubber/composite hybrid structure, Composite structures, 113 (2014), 469-475.

[25] I. Finnie, Erosion of surfaces by solid particles, Wear. 3 (1960), 87-103.

[26] J.H. Neilson, A. Gilchrist, Erosion by a stream of solid particles, Wear. 11 (1968), 111-122

[27] M. Lindroos, M. Apostol, V-T. Kuokkala, A. Laukkanen, K.Valtonen, K. Holmberg, O. Oja, Experimental study on the behavior of wear resistant steels under high velocity single particle impacts, International Journal of Impact Engineering. 78 (2015), 114-127.

[28] Y.I. Oka, H. Ohnogi, T. Hosokowa, M. Matsumura, The impact angle dependence of erosion damage caused by solid particle impact, Wear. 203-204 (1997), 573-579

[29] P.H. Shipway, S.J. Wood, A.H. Dent, The hardness and sliding wear behaviour of a bainitic steel, Wear. 203-204 (1997), 196-205.

[30] R.W. Fricke, C. Allen, Repetitive impact wear of steels, Wear. 162-164(1993), 837-847.

[31] M. Lindroos, K. Valtonen, A. Kemppainen, A. Laukkanen, K. Holmberg, V-T. Kuokkala. Wear behavior and work hardening of high strength steels in high stress abrasion, Wear. 322-323 (2015), 32-40

[32] Z.X. Yin, C.M. Ma, S.X. Li, G.Q. Cheng, Perforation of an ultra-high strength steel penetrated by sharped charge jet, Materials Science and Engineering A. 379 (2004), 443-447.

[33] M.N., Bassim, A.G. Odeshi, Shear strain localization and fracture in high strength structural materials. Archives of Materials Science and Engineering. 31 (2008) 2, 69-74.

[34] Z.Q. Duan, S.X. Li, W. Huang, Microstructures and adiabatic shear bands formed by ballistic impact in steels and tungsten alloys. Fatigue & Fracture of Engineering Materials & Structures. 26 (2003) 12, 1119-1126.

[35] W. Molnar, S. Nugent , M. Lindroos, M. Apostol, M. Varga, Ballistic and numerical simulations of impacting goods on conveyer belt rubber, Polymer Testing. 42 (2015), 1-7.

[36] M. Lindroos, M. Apostol, V. Heino, K. Valtonen, A. Laukkanen, K. Holmberg, V-T. Kuokkala. The deformation, strain hardening, and wear behavior of chromium alloyed Hadfield steel in abrasive and impact conditions, Tribology Letters. 57 (2015) 3, 1-11.

[37] P. Suikkanen, J. Kömi, Microstructure, Properties and Design of Direct Quenched Structural Steels, Materials Science Forum. 783-786 (2014), 246-251.